

Spaceborne millimeter wavelength cloud radar reflectivity factor simulation

Huifa Liu*, Wei Yan*, Ding Han*, Rui Wang*

*College of Meteorology and Oceanography, PLA University of Science and Technology, Nanjing, China
liuhuifa@gmail.com, weiyanyan2002net@yahoo.com, handing_ok@126.com, wanggruissw@126.com

Abstract—The Simulation of millimeter wavelength cloud radar reflectivity factor, which aimed to verify the inversion algorithm of cloud microphysical parameters, is an important issue in millimeter wavelength cloud radar development and the validation of its performance. By using the auxiliary data of temperature, humidity and pressure published by European Centre for Medium-Range Weather Forecasts, the simulation calculates the droplet size distribution parameters of each bin along the CloudSat satellite's sounding profiles, which may follow lognormal distribution or power-law distribution. Then every single particle's backward scattering efficiency and attenuation efficiency are computed in Mie scattering model, the number concentrations and sizes of these particles are finite, and then the reflectivity and attenuation coefficient of each bin get calculated. After the attenuation correction, the observed and simulated radar reflectivity are compared. The consequence shows that the outcome of simulation is in good agreement with actual sounding data.

Keywords—MMW cloud radar; simulation; Mie scattering

I. Introduction

Millimeter wavelength (MMW) cloud radar is an important part of modern meteorological radars, which has so many advantages that can not be replaced by other sensors. Major domestic and foreign manufacturers devote lots of energy to develop MMW cloud radar detection technology, in order to obtain the cloud microphysical parameters and cloud structure. MMW cloud radar is small and light to be boarded in vehicle, airborne and spaceborne platforms. One of the most famous cases is the United States' CloudSat satellite carrying the cloud profiling radar (CPR).

In America and Europe, MMW cloud radar detection technology has been working for decades, while our national airborne and spaceborne MMW cloud radars are still in intensive developing. It needs large amount of experiments and simulations to validate the radar's performance and the validity and accuracy of inversion algorithms. With the rapid advancement of military science and technology, simulation has become an indispensable method for varieties of complex system development. Many researchers performed a series of simulations for meteorology radars respectively. Wu Qiong[1] at al used the Quickbeam simulator package to find the optimum frequencies for FY-3 satellite project, confirming Ku wave band and Ka wave band as the FY-3 satellite's working frequency in rainfall detection. Wu Renbiao[2] at al designed an airborne weather radar echo generation and signal

presentation simulation system, mainly used in the radar echo simulation of the wind field data. Sun Xianming[3] at al used Monte Carlo method to calculate the vertical microscopic characteristics of continuous changing rainfall melting layer on different frequency electromagnetic wave's reflectivity. But these researches are only applied to weather radar or wind profiling radar, or only in response to a single weather phenomenon just like rainfall melting layer without considering the measured data and background data. So we combined CloudSat sounding data and European Centre for Medium-Range Weather Forecasts (ECMWF) data, using the forward model of CloudSat data retrieval algorithm to simulate the spaceborne MMW cloud radar and then took the Lidar data as auxiliary data to compare the simulation outcome with the actual sounding data.

Furthermore, three issues are considered: (1)The algorithm should be efficient and fast, but doesn't require a realtime operation; (2)The simulator doesn't contain all the actual observation and calibration processes such as the satellite attitude correction, calibration coefficient correction etc. (3) Radar parameters like transmitter power, antenna gain, beam width aren't considered except wavelength, dielectric constant.

II. Data Analysis

CloudSat Data Processing Center (DPC) distributions level 1B products and level 2B products. Level 1B products are standard raw data with simple geographic calibration and transmission error correction, such as the calibration of radar backscattering profile (1B-CPR), CPR raw data (1A-AUX); Level 2B products are based on level 1B, Aqua satellite's Moderate Resolution Imaging Spectroradiometer (MODIS) product, CALIPSO satellite cloud-aerosol lidar with orthogonal polarization (CALIOP) product and ECMWF product, which are joint together as auxiliary data.

As mentioned above, the 2B-GEOPROF product is the cloud geometric profile with atmospheric attenuation correction according to the Significant Echo Mask (SEM) algorithm proposed by Mace[4]. Using the CloudSat/CPR 1B products as input and separating the useful radar echo to generate cloud geometric radar backward reflectivity factor. The 2B-GEOPROF-LIDAR product combines CPR data and Lidar data, giving the number of cloud layer and the corresponding cloud top height. Due to CALIOP has a higher vertical resolution and sensitivity to tenuous clouds and thin

ice clouds which have a low optical depth, the 2B-GEOPROF-LIDAR product uses CALIOP observations to determine cloud top height[5]. The ECMWF-AUX[6] distributed by ECMWF contains temperature, humidity and pressure data, which was interpolated from ECMWF meteorological data to the CloudSat sounding units. The simulation takes the temperature profile, humidity profile and pressure profile as inputs and then calculates the modelling radar reflectivity factor (Table I).

TABLE I. THE PARAMETERS OF THE SIMULATION PROGRAM

Input	Intermediate variables	Output
Humidity	Particle size Particle phase Air density Complex refractive index Back scattering ratio	Radar reflectivity factor
Temperature		
Pressure		

III. Steps And Theories Of The Simulator

A. Cloud layer distinguish

Wang[7] et al analyzed radiosonde and ground-based observations statistically and concluded that the frequency distribution of the cloud base humidity had a significant change around 87%, while only 1/4 of clouds whose humidity was greater than 84% existed in all samples. So we take 87% as the threshold to determine the presence of clouds. For each sounding profile, the simulation will be processed where clouds exists.

B. Particle phase

Polarization radar echo could identify cloud phase accurately, but CloudSat can not offer polarization information[8]. So temperature threshold was used to be the effective method to identify cloud phase. When the temperature is greater than 0°C, the cloud phase is liquid, when the temperature is less than -40°C, the cloud phase is ice, otherwise the phase is mixed-phase[9].

C. Air density and particle density

Hydrometeor particle density may be either specified as a constant or it can be expressed as a function of diameter. The mass-diameter relation is given by

$$m(D) = \alpha_m D^{\beta_m}, \quad \alpha_m, \beta_m > 0 \quad (1)$$

If the density is specified to a constant, α_m and β_m should be set to -1, if not, α_m and β_m should be set to constants, usually $\beta_m = 3$ for liquid and $\beta_m < 3$ for ice. The air density is given by

$$\text{Dry air: } \rho_a = \rho_0 \cdot \frac{273}{273+t} \cdot \frac{P}{0.1013} \quad (2)$$

$$\text{Wet air: } \rho_a' = \rho_0 \cdot \frac{273}{273+t} \cdot \frac{P - 0.0378e}{0.1013} \quad (3)$$

with $\rho_0 = 1.293 \text{ kg/m}^3$, the air density at 0°C, 0.1013Mpa.

e is vapor pressure. P is atmosphere press, t is centigrade temperature. ρ_a is the density of dry air and ρ_a' is the density of wet air. Equation (3) can be simplified to

$$\rho_a = \frac{100P}{287 * (t + 273)} \quad (4)$$

D. Drop-Size Distribution

Drop-size distribution (DSD) refers to the number-size distribution of cloud droplets per volume. The unit of cloud droplet concentration, which is also called cloud droplet numeric density, is usually described by cm^{-3} , meaning the number of droplets per volume. With the character parameters like distribution width, concentration peak and radius peak. The concentration increases with droplet getting bigger before reaching the peak and then declines, and the peak usually occurs while the radius is small relatively. These parameters change with area, cloud type, regions in cloud and the period of cloud (Table II)[10]. There are two distribution models as follows:

TABLE II. THE PARAMETERS OF EXPONENTIAL FORMULA

Type	$N(\text{cm}^{-3})$	ν	r_c	$n(r_c)$
Haze M	100	1/2	0.05um	$360.9 \text{ cm}^{-3} \text{ um}^{-1}$
Rain M	1000	1/2	0.05mm	$3609 \text{ m}^{-3} \text{ mm}^{-1}$
Haze L	100	1/2	0.07um	$446.6 \text{ cm}^{-3} \text{ um}^{-1}$
Rain L	1000	1/2	0.07mm	$4466 \text{ m}^{-3} \text{ mm}^{-1}$
Haze H	100	1	0.10um	$541.4 \text{ cm}^{-3} \text{ um}^{-1}$
Hail H	10	1	0.10cm	$54.14 \text{ m}^{-3} \text{ cm}^{-1}$
Cumulus C.1	100	1	4.00um	$24.09 \text{ cm}^{-3} \text{ um}^{-1}$
Corona C.2	100	3	4.00um	$49.41 \text{ cm}^{-3} \text{ um}^{-1}$
Fritillaria C.3	100	3	2.00um	$98.82 \text{ cm}^{-3} \text{ um}^{-1}$

1) Lognormal distribution

The lognormal distribution[11] is defined as

$$n(r) = \frac{N_t}{\sqrt{2\pi\sigma_{\log}^2} r} \exp\left[-\frac{\ln^2(r/r_g)}{2\sigma_{\log}^2}\right] \quad (5)$$

N_t is the total droplet numerical density, r is droplet radius, $r_g, \sigma_{\log}, \sigma_g$ are given by

$$\ln r_g = \overline{\ln r}, \quad \sigma_{\log} = \overline{\ln \sigma_g}, \quad \sigma_g^2 = \overline{(\ln r - \ln r_g)^2}$$

Where r_g is the geometric mean particle radius, σ_{\log} is the distribution width, σ_g is the geometric standard deviation. \ln means natural logarithm.

2) Power law distribution

The power law distribution[12] is defined as

$$n(r) = \frac{N_t}{\sqrt{2\pi\sigma_{\log}^2} r} \exp\left[-\frac{\ln^2(r/r_g)}{2\sigma_{\log}^2}\right] \quad (6)$$

This model is available for ice particles only. D is the diameter of ice particle, A_r is distribute constant, b_r is the function of temperature t (Table III).

TABLE III. THE RELATIONSHIP BETWEEN b_r AND t

Temperature $t^\circ\text{C}$	Cloud type	b_r
< -30	Cirrus	$-1.75+0.09(t-32.99)$
-30 — -9	Cirrus	$-3.25-0.06(t-10.49)$
-9 — 0	Cirrus	-2.15
< -35	Frontal	$-1.75+0.09(t-32.99)$
-35 — -17.5	Frontal	$-2.65+0.09(t-20.49)$
-17.5 — -9	Frontal	$-3.25-0.06(t-11.49)$
-9 — 0	Frontal	-2.15

E. Mie scattering calculating

The wavelength of MMW cloud radar is as the same magnitude as the size of cloud particles. So Mie scattering model are more accurate according to the scattering theory. All the cloud droplets are modeled as “soft sphere” in this simulation, and multiple scattering is neglected. In the classic Mie scattering theory, the backscattering efficiency Q_b and attenuation efficiency are given by

$$Q_b = \frac{1}{\alpha^2} \left| \sum_{n=1}^{\infty} (-1)^n (2n+1)(a_n - b_n) \right|^2 \quad (7)$$

$$Q_a = Q_e + Q_s \quad (8)$$

Where

$$Q_e = \frac{2}{\alpha^2} \sum_{n=1}^{\infty} (2n+1) \text{Re}(a_n + b_n) \quad (9)$$

$$Q_s = \frac{2}{\alpha^2} \sum_{n=1}^{\infty} (2n+1)(|a_n|^2 + |b_n|^2)$$

Q_e is the extinction efficiency, Q_s is the scattering efficiency. Size parameter $\alpha = 2\pi r/\lambda$, a_n , b_n are Mie scattering parameters, which are the function of α and complex index of refraction $m(=n'+j \cdot n'')$ with Bessel function and Hankel function. The Mie scattering calculating module[13] distributed by the department of physics in Oxford University was called in the simulator.

F. Calculating radar reflectivity factor

Using the backscattering efficiency and extinction efficiency in (10), the reflectivity and attenuation coefficient can be calculated by summing all the particles’ backscattering cross-section and attenuation coefficient as

$$\eta = \sum_{all} \sigma_{bi} = \sum_{all} Q_{bi} \pi r_i^2 \quad (10)$$

$$\alpha = \sum_{all} \sigma_{ai} = \sum_{all} Q_{ai} \pi r_i^2 \quad (11)$$

η is reflectivity, σ_{bi} is the radar backscattering cross-section of the particle with the size r_i . α is the attenuation coefficient, σ_{ai} is the attenuation coefficient of the particle with the size r_i . The radar reflectivity factor is given by

$$z = \frac{\lambda^4 \eta}{\pi^5 |K|^2} 10^{18} \quad (12)$$

$|K|^2$ is complex permittivity, which equal 0.75 when the radar wavelength $\lambda = 3$ mm.

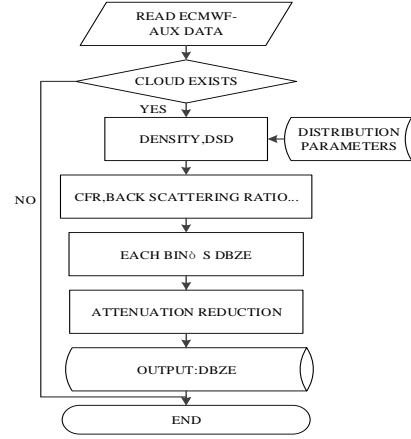


Fig.1. The simulation flowchart

IV. Low Clouds Weather Process Radar Echo Simulation And Analysis

A low clouds weather process was sounded by CloudSat around (53.5 S-61.0 S, 53 W-63 W) in February 25, 2009. The effective radar reflectivity presented in Fig.2 had been processed with significant echo mask(SEM), denoising and attenuation correction. The output of simulation was shown in Fig.3. It’s obviously that the simulation products are in great consistent with the clouds’ geometric contours below 5km while the difference getting larger above 5km, as shown in the red box, in this area, the radar reflectivity is -20dBz ~ -5dBz in simulation but none in actual sounding product. To evaluate the outcome, the cloud top sounded by the CALIPSO satellite was plotted in Fig.3, which shows the simulation outcomes are more accurate. This phenomenon is usually caused by the weakness of MMW radar: low sensitive to tiny ice cloud which can be detected by the short wavelength sensitive like lidar. In general, the simulator can provide lots of valuable and accurate information.

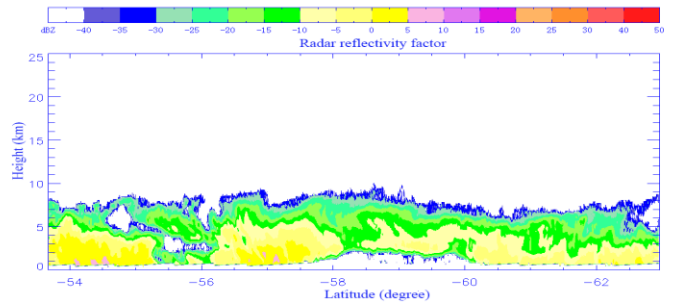


Fig.2. The observed radar reflectivity

The error between the simulated and observed product may come from three sources: (1) the radar measurement error; (2) algorithm error, which is caused by approximate calculation and model simplification; (3) data matching error, which is caused when many kinds of products are combined and interpolated to the CloudSat data format. All the errors are counted in (13) as a whole. The simulated vs. observed

contrast diagram is shown in Fig.4, and the error distribution histogram is shown in Fig.5.

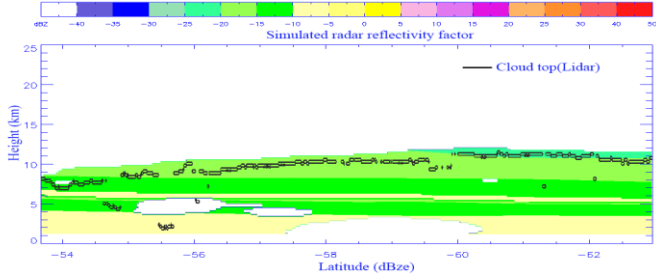


Fig.3. The simulated radar reflectivity

$$\sigma(Z_{dBz})_{MD} = \frac{\sum_{i=1}^n |Z_{dBz} - Z'_{dBz}|}{n} \quad (13)$$

$$\sigma(Z_{dBz})_{SD} = \sqrt{\frac{\sum_{i=1}^n (Z_{dBz} - Z'_{dBz})^2}{n}}$$

Z_{dBz} and Z'_{dBz} are simulated and observed reflectivity factor separately, $\sigma(Z_{dBz})_{MD}$ and $\sigma(Z_{dBz})_{SD}$ are denoted as average deviation and standard deviation. For the low clouds simulation, the average deviation is 3.34dBz, and the standard deviation is 7.53dBz.

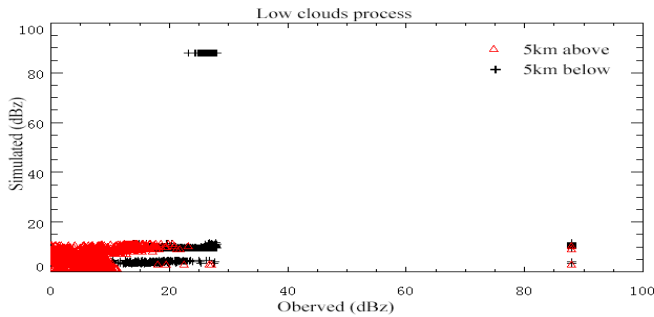


Fig.4. The simulated vs. observed contrast diagram

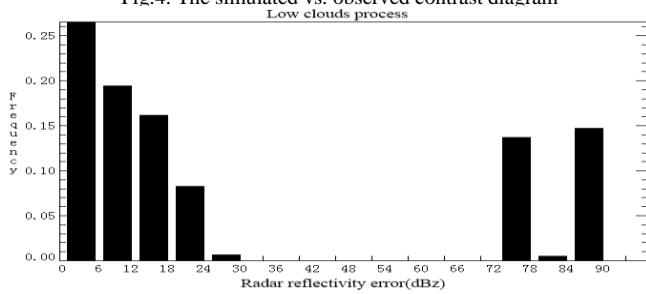


Fig.5. The error distribution histogram

V. Conclusions And Discussions

The following conclusions can be drawn by comparing the observed and simulated low clouds weather process on February 25, 2009: The MMW radar has a weak capability in tiny ice clouds detection, which can be detected by the lidar in CALIPSO satellite and exist in the outcome of simulation. The altostratus simulation results are more accurate than the low clouds. Besides, due to the low resolution of the ECMWF data,

the simulation results are presented on the vertical distribution of stratification, and can not reach the fine results observed by CPR radar.

Furthermore, the satellite Aqua carries a high resolution sensor "The Humidity Sounder for Brazil (HSB)", which can provide more accurate data needed to the simulator, but unfortunately, this equipment turned into breakdown soon when the satellite was transmitted. To our national MMW cloud radar program, it's advised to equip a microwave humidity radiometer jointed to the MMW cloud radar in order to achieve a more accurate cloud microphysical structure by joint exploration.

VI. Acknowledgment

Thanks are due to NASA CloudSat DPC for offering the data used in this study. This work is supported by the National Natural Science Foundation of China (Project 41076118) and they National Natural Science Foundation of China (Project 41005018).

VII. References

- [1] Wu Qiong, Yang Hu, "Spaceborne precipitation Lu Maimeng. radar frequency band selection simulation study," Journal of Meteorology, vol. 69, no. 2, pp. 344–351, 2011.
- [2] Wu Renbiao, Hu Pengju, Lu Xiaoguang, "Airborne weather radar echo signal simulation system," Journal of Civil Aviation University of China, vol. 30, no. 2, pp. 1–5, 2012.
- [3] Sun Xianming, Han Yiping, Shi Xiaowei, "Monte Carlo simulation of backscattering by a melting layer of precipitation," Journal of China, vol. 56, no. 4, pp. 42–40, 2007.
- [4] G. Mace, "Level 2 GEOPROF product process description and interface control document algorithm version 5.3," NASA Jet Propulsion Laboratory, 2007.
- [5] W. Zhien, S. Kenneth, V. Deborah, and others, "Level 2 Combined Radar and Lidar Cloud Scenario Classification Product Process Description and Interface Control document," CloudSat Project Jet Propulsion Laboratory, Pasadena California, 2003.
- [6] R. Austin, "CloudSat ECMWF-AUX auxiliary data process description and interface control document, version 5.2.," CloudSat Data Processing Center, 2007.
- [7] W. Zhien and S. Kenneth, "Cloud Type and Macrophysical Property Retrieval Using Multiple Remote Sensors," Journal of Applied Meteorology, vol. 40, pp. 1665–1682, 2001.
- [8] Yan Wei, Ren Jianqi, Lu Wen, et al, "The spaceborne millimeter wave radar and lidar consistent data cloud phase recognition technology," Journal of infrared and millimeter waves, vol. 30, no. 1, pp. 68–73, 2011.
- [9] Z. Wang and K. Sassen, "Level 2 cloud scenario classification product process description and interface control document," Cooperative Institute for Research in the Atmosphere, 2007.
- [10] Sheng Peixuan, Mao Jietai, Li Jianguo, et al, Atmospheric Physics. Beijing: Peking University Press, 2003.
- [11] R. T. Austin and G. L. Stephens, "Retrieval of stratus cloud microphysical parameters using millimeter-wave radar and visible optical depth in preparation for CloudSat 1. Algorithm formulation," J. Geophys. Res., vol. 106, no. D22, pp. 28233–28242, Nov. 2001.
- [12] B. F. Ryan, "A bulk parameterization of the ice particle size distribution and the optical properties in ice clouds," Journal of the atmospheric sciences, vol. 57, no. 9, pp. 1436–1451, 2000.
- [13] Department of Physics, Oxford, London, "mie_single.pro," 27-Jul-2012. [Online]. Available: http://www.atm.ox.ac.uk/code/mie/mie_lognormal.html.